Low-Pressure Plasma Spectroscopic Diagnostics

T. L. Eddy*
Georgia Institute of Technology, Atlanta, Georgia 30332

Diagnostic techniques have recently been developed that permit the determination of the deviation from local thermal equilibrium (LTE) in subatmospheric electric arcs and plasma jets. A review is presented of the methods that are applicable to MPD (magnetoplasmadynamic) and arcjet thruster plasmas but that have not been used in space propulsion research. Appropriate plasma diagnostics can lead to increased thrust, better nozzle design, and improved modeling capabilities. These methods include nonintrusive techniques, and can determine the electron, T_e, gas, T_g, and total excitation, T_{exa}, temperatures, as well as the electron and atom densities, without using LTE or partial LTE assumptions. General relations for analysis and experimental results for argon constricted arcs, an arc in a rotating magnetic field, and plasma torch jets are presented. The methods discussed can also be applied to plasma mixtures.

Nomenclature

A_{mn} = transition probability from level m down to level n
c = speed of light
D_a = ambipolar diffusion coefficient
E_f = electric field strength
E_l, E_∞ = lowered and original ionization energy ($E_l = E_\infty - \Delta E_\infty$)
E_m, E_n = energy of upper and lower electronic levels
G_f = free-free Gaunt factor
g_m, g_n = degeneracy of upper and lower electronic levels
H = enthalpy
h = Planck constant
k = Boltzmann constant
k_e, k_g = thermal conductivity for electron, gas
m_e, m_g = mass of electron and gas particle
N_a, N_e, N_i = species number density: atoms, electrons, ions
N_m, N_n = number densities of electronic levels m and n
p = pressure
Q_{ea}, Q_{ei} = collision cross sections: electron-atom, electron-ion
r = radius
T_{exa} = total electronic excitation temperature between ground state and highest excited level of atom [see Eq. (1)]
$T_{ex\beta}$ = upper level electronic excitation temperature
T_g = gas or heavy particle translation temperature
$T_{\rm LTE}$ = temperature calculated under the LTE assumption, usually using emission lines from high lying levels
$T_{\rm norm}$ = temperature at the normal point located at the peak value of the emission coefficient (versus temperature) at constant pressure
$T_{\rm ratio}$ = equivalent to $T_{ex\beta}$
u = average velocity between positions 1 and 2
Z_{exa}, Z_{exi} = electronic partition functions of the atom and ion
z = charge of the species (=1 here)
γ = degeneracy or multiplicity of the ground state of the ion
ΔE_s = advance of series limit[5]
ΔE_∞ = lowering of the ionizational potential[5]
λ = wavelength
ν = frequency
σ = electrical conductivity

Presented as Paper 89-2830 at the AIAA/ASME/SAE/ASEE 25th Joint Propulsion Conference, Monterey, CA, July 10–12, 1989; received July 9, 1990; revision received Nov. 28, 1990; accepted for publication Dec. 6, 1990.

*Associate Professor; currently Principal Engineer, Plasma Processing, Idaho National Engineering Laboratory/EG&G Idaho, Inc., P.O. Box 1625, Idaho Falls, Idaho 83415-2210. Member AIAA.

Introduction

A VARIETY of experimental measurements on magnetoplasmadynamic (MPD) and arcjet thruster plumes has raised questions about actual species densities: 1) electron, ion, and gas temperatures and 2) velocity and flow conditions in the nozzle and plume. At pressures below atmospheric, deviations from local thermal equilibrium (LTE) are expected. The exact form of these deviations is not well understood. This paper presents results from non-LTE plasma studies in the vicinity of 1-atm which have resulted in consistency between various relations and a better understanding of the non-LTE thermodynamics. If we do not understand the thermodynamics, we cannot do the proper bookkeeping for the heat transfer and fluid dynamics.

For simplicity, the present work considers a monatomic plasma with one level of ionization, i.e., argon, first argon ions, and electrons. The methods are relatively easily applied to multicomponent or multiply ionized plasmas that may also be diatomic or polyatomic. Simplifications appropriate to these complex plasmas need to be determined experimentally.

The types of non-LTE considered here have been demonstrated by theory or experiment. It is an accepted fact that at sufficiently high densities, but significantly below atmospheric pressure, the distribution of heavy particle (atom, ion, or gas) and electron translational energies is Maxwell-Boltzmann, but the distribution parameter T may have different values; hence, $T_g \neq T_e$. It has also been shown experimentally that one cannot expect the highly excited energy levels to be populated according to T_e,[1] but that these levels are often found to be related by one temperature: $T_{ex\beta} = T_{\rm ratio} \neq T_e$. Note that the term partial LTE or PLTE is often used, assuming that 1) $T_{ex\beta}$ follows a Boltzmann distribution over the highest levels and 2) $T_{ex\beta} = T_e$. When Assumption 2 is not included, then, and only then, is the PLTE model appropriate. Another type of non-LTE is shown by radiative-collisional calculations[2–4] in which the ground state density is not populated at the temperature of the upper levels, $T_{exa} \neq T_{ex\beta}$. The total excitation or ionization temperature, T_{exa}, is defined by

$$N_l/g_l = (N_{1,a}/g_{1,a}) \exp(-E_{l,a}/kT_{exa}) \tag{1}$$

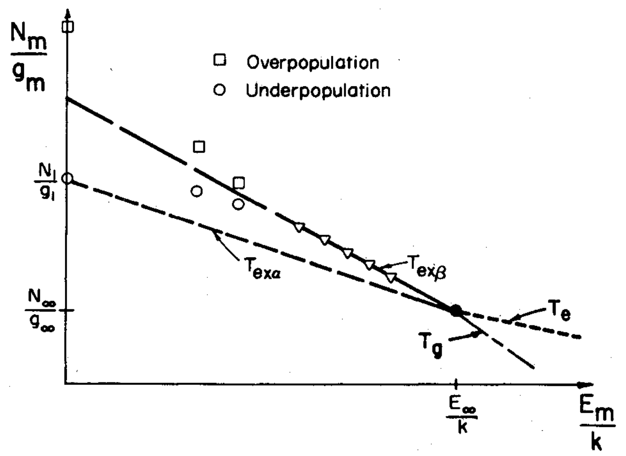

Fig. 1 Boltzmann plot of meaningful plasma temperatures.[6]

where N_l and g_l are the effective number density and degeneracy of the highest excited level determined by the intercept at the lowered ionization energy $E_{l,a}$. $N_{1,a}$ and $g_{1,a}$ are the corresponding terms at the ground state. The ionization potential is lowered using the methods of Griem.[5]

The four resulting temperatures, illustrated in Fig. 1, are sufficient to describe the thermodynamic state in a monatomic, singly-ionized plasma. The particular multitemperature model applied here is called the generalized multithermal equilibrium (GMTE) model,[7] in which the temperatures are physically meaningful. T_e and T_g as translational temperatures are important in determining transport properties, dominate the conservation equations, and are the main indicators of energy storage, e.g., via enthalpy. $T_{ex\beta}$ is determined from spectral line intensity measurements and the Boltzmann factors

$$N_m/g_m = (N_n/g_n)\exp[-(E_m - E_n)/kT_{ex\beta}) \tag{2}$$

$T_{ex\beta}$ is the temperature for the optically thin radiation emitted from the plasma, is used to extrapolate for N_l/g_l, and plays an important role in the continuum relation as shown later. T_{exa} is a very important temperature that is often overlooked. It is the temperature to be used in the electronic partition function, Z_{exa}, and can be used to estimate the temperature of the resonance line radiation. More importantly in diagnostics (and modeling), it provides the link between the measurable excited level densities and the difficult to measure atom density via Eq. (1) and

$$N_a/Z_{exa}(T_{exa}) = N_{1,a}/g_{1,a} \tag{3}$$

We also find in plasma jets that the non-LTE appears to be mainly due to over- or under population of the ground state ($T_{exa} \neq T_e$) and not the usually assumed kinetic nonequilibrium ($T_g \neq T_e$). The reason appears to be that equilibration between excited electronic levels and the ground state is slower than the equilibration between translational energies of the free electrons and heavy particles. In the plume, the absence of significant electric field strengths will not elevate the electron translational temperature above the gas temperature. Near the plasma boundaries, gas conduction has been shown to exceed electron loss mechanisms[8,9] that can result in $T_e > T_g$.

An explicit comparison of the GMTE and some PLTE type models using the collisional-radiative (C-R) modeling technique in hydrogen[4,10,11] shows that both methods predict similar N_e vs T_e, but differ significantly in predicting atom or ground state densities. The comparison also shows that departure coefficients do not go to unity with increasing energy level, unless $T_g = T_e$ (kinetic equilibrium). This is another contradiction because in real plasmas, it is often assumed that the non-LTE comes from or is related to $T_g < T_e$ and that departure coefficients do go to unity. Finally, the comparison shows that the "analytic" GMTE model used for diagnostics gives identical results (for species densities) as the detailed multilevel "collisional-radiative" GMTE model; therefore, the analytic GMTE model can be used with confidence for diagnostics or modeling.

Below, we present the non-LTE equations for diagnostics and a description of experiments on arcs with and without magnetic fields and plasma jets in which these diagnostic methods have been applied. In addition to some low-temperature approximations, four medium temperature methods are discussed. The ARCS program was developed in Fortran on a CDC Cyber[7,9,12–14] for use in constricted or free-burning arcs where the electric field strength is significant and known. It was later modified for HP BASIC[15] and IBM PC/AT/PS-2 Fortran at INEL. The TETG, JET-G and JET-H programs were developed in HP BASIC.[15] TETG and JET-G have been converted to PC Fortran at INEL. TETG assumes kinetic equilibrium ($T_e = T_g$) and, thereby, eliminates the need for the energy equations. The JET programs are for field free-plasma plumes. JET-G is a local "differential" type of analysis which obtains the difference between T_e and T_g from the difference in energy loss from their respective translational energy reservoirs. JET-H actually performs the energy balance between two axial cross sections, complete with velocity profiles et al. Technical details of the programs are given below.

Theory

General Equations

A minimum complexity of experimental measurements is desired; hence, easily measured line and continuum intensities are often the source for excited level populations and the electron density. Laser induced fluorescence (LIF) or Rayleigh scattered laser (RSL) methods could be used in addition to or in place of emission measurements. The excited level number density, N_m, is obtained from the line emission coefficient, i_L, (after performing the Abel inversion on the net line intensity)

$$i_L = (hc/4\pi\lambda)A_{mn}N_m \tag{4}$$

$T_{ex\beta}$ is then obtained from Eq. (2) using two or more lines in a least squares fit. The intercept N_l/g_l is obtained at the same time. The values of pressure p, N_m's, $T_{ex\beta}$, and N_l/g_l are now known explicitly for this analysis. For low-pressure plume analysis, the static pressure will need to be measured or treated as an additional unknown.

The assumptions for the equations used are: Maxwellian velocity distributions for the heavy particles (nonelectrons) at T_g, Maxwellian velocity distribution for the free electrons at T_e, quasineutrality ($N_e = N_i$), $T_{exi} = T_{exa}$ in the partition functions because T_{exi} plays a minor role, and $T_c = T_{ex\beta}$ for reasons discussed in Ref. 16. The ionization (Saha-Eggert) relation, Eq. (8) below, is an extension of the two-temperature Saha relation to include the effect of over- or underpopulation of the ground state. The equation is rigorously derived on the basis of Boltzmann energy distributions for each energy mode (translational, electronic) at its own distribution parameter (temperature), (thermal nonequilibrium) and chemical equilibrium. The assumed temperature equivalences indicated above are used to simplify the equation to the form shown.

The unknowns are N_e, N_a, T_e, T_g, and T_{exa}, since we can assume quasineutrality ($N_e = N_i$) here. The five equations used to calculate the five unknowns are selected from the following general equations. GMTE continuum relation (mainly for N_e)[7,17,18] is

$$\varepsilon_\nu = 5.44 \times 10^{-46}\, z^2 N_e N_i T_e^{-1/2}\, \xi \exp(-\Delta E_\infty/kT_{ex\beta}) \tag{5}$$

where

$$\xi = G_f \exp[(\Delta E_s - h\nu)/kT_e] + (\beta_c T_{ex\beta}/T_e)(1.4\gamma/Z_{exi})\xi_{fb}(\nu, T_{ex\beta})\cdot[1 - \exp(h\nu/kT_c)]$$

$$\beta_c = [N_e/2(2\pi m_e kT_e/h^2)^{3/2}]^{(T_e/T_g)-1} \cdot[(Z_{exa}/Z_{exi}) \exp(E_{I,a}/kT_{exa})]^{(T_{exa}/T_g)-1}$$

and ξ_{fb} is the free-bound ξ factor from Schluter[18] or similar source at the frequency and $T_{ex\beta}$. We also use the good assumption that the recombination continuum temperature, T_c, equals $T_{ex\beta}$.[16] The $(\beta_c T_{ex\beta}/T_e)$ factor is the major non-LTE correction factor. The $1.4\gamma = 1.4g_{1,i}$ factor accounts for the apparent omission of the $2g_{1,i}$ factor in lieu of $1\ g_{1,i}$ in the original formulation (compare Refs. 5 and 10), that results in a factor of two difference between high-pressure experimental free-bound factors and theoretical values.[16] Corrected A_{mn} by Sedghinasab[7,12] makes a 70% correction factor; hence, 70% times two yields the 1.4 factor. Without this (or a slightly larger) factor, the solution at high temperatures near the nozzle exit yields higher electron densities than possible. With this correction to the theoretical free-bound factors, consistency is obtained between $H\beta$ Stark broadening, argon continuum (near 4400 A), and the Sedghinasab A_{mn} scale for N_e determination in high-pressure LTE and non-LTE experiments.[15]

Total Boltzmann distribution, a combination of Eqs. (1) and (3) is

$$N_a = Z_{exa}(N_I/g_I) \exp(-E_{I,a}/kT_{exa}) \tag{6}$$

Equation of state

$$p = (N_a + N_i)kT_g + N_e kT_e \tag{7}$$

GMTE ionization (Saha-Eggert) relation is[7,10]

$$N_e(N_i/N_a)^{T_g/T_e} = 2\,\frac{2\pi m_e kT_e^{3/2}}{h^2}\,\frac{Z_{exi}^{\;T_{exa}/T_e}}{Z_{exa}}\,\exp\frac{-E_{I,a}}{kT_e} \tag{8}$$

Electron energy relation[8,9]

$$Q_{e-\mathrm{cond}} + Q_{e-\mathrm{amb}} + Q_{e-\mathrm{rad}} + Q_{eq} + W_e = \Delta H_e \tag{9}$$

where

$$Q_{e-\mathrm{cond}} = (1/r)d[rk_e(dT_e/dr)]/dr$$

$$Q_{e-\mathrm{amb}} = (5kT_e/2r)d[rAD_a(dN_e/dr)]/dr$$

$$A = [N_a/(N_a + N_e)][1 - (N_e/N_a)(dN_a/dN_e)] \simeq 1$$

$$Q_{eg} = C_{eg}(T_g - T_e),\ W_e = \sigma E_f^2$$

$$C_{eg} = (3m_e/m_g)kN_e(3kT_e/m_e)^{1/2}(N_e Q_{ei} + N_a Q_{ea})$$

$$\Delta H_e = (5k/2)(T_{e,2}N_{e,2} - T_{e,1}N_{e,1})(u/\Delta x)$$

$Q_{e-\mathrm{rad}}$ is estimated from LTE values.[19] The error from this inconsistency is negligible at low pressures (<1 atm) because the $Q_{e-\mathrm{rad}}$ contribution is small.[9] It is found that T_{exa} is the "LTE" temperature to be used for the present conditions. Subscripts 1 and 2 indicate cross sections that are Δx apart.

Gas energy equation is

$$Q_{g-\mathrm{cond}} + Q_{ge} = \Delta H_g \tag{10}$$

where

$$Q_{ge} = -Q_{eg},\ = C_{eg}(T_e - T_g)$$

$$Q_{g-\mathrm{cond}} = (1/r)d[rk_g(dT_g/dr)]dr$$

and at each x location

$$H_g = (5/2)kT_g(N_a + N_i) + N_i E_{I,a}$$

The LTE properties calculated are based on the line with the highest energy level unless otherwise indicated. The method of solution differs with each diagnostic technique as discussed later.

Low-Temperature Approximations

Several low-T methods have been proposed which reduce the number of equations required when the temperature (T_{exa}) is sufficiently below the normal temperature. These low-T approximations are obtained from plots of the non-LTE thermodynamic properties calculated with the GMTE model relations. The first approximation[20] says that if $T_{exa} << T_{\mathrm{norm}}$, then

$$T_{exa} = T_{\mathrm{LTE}}(i_L \text{ or } N_m) \tag{11}$$

which means that T_{exa} can be found from the LTE temperature. It follows from the fact that all non-LTE i_L converge to the LTE curve at temperatures sufficiently below the normal temperature, T_{norm}, for a given spectral line when plotted vs T_{exa} (but not when vs T_e) as shown in Fig. 2. This is a very desirable result, because if N_I/g_I is obtained via Eq. (2) and T_{exa} from Eq. (11), then N_a is easily determined from Eq. (6). Early attempts to use this approximation were not successful in predicting reasonable T_g. A more detailed study[15] has shown that the approximation is sufficiently accurate to predict densities only at T_{LTE} much lower than $T_{\mathrm{LTE,norm}}$ because of the relatively strong nonequilibrium usually found. For a 20% accuracy in N_a, $|T_{exa} - T_{\mathrm{LTE}}| \leq 100$ K for a typical argon, hydrogen, or nitrogen plasma.

The second approximation,[15] resulting in Eqs. (12) and (13),

$$T_e = T_{\mathrm{LTE}}(N_e) \tag{12}$$

$$N_a = N_e/(N_i/N_a) = N_a[T_{\mathrm{LTE}}(N_e)] \tag{13}$$

is obtained from the state diagram, such as shown in Fig. 3 for hydrogen. At one pressure, when $T_e = T_g$, it can be seen that all T_e/T_{exa} curves lay on top of the LTE curve, at the same T_e value, while T_{exa} changes in value. This means that measured N_e can be used to estimate T_e and N_a from Eqs. (12) and (13). Though this method has not been used to our knowledge, it appears to have many advantages in plasma jet applications (where $T_g = T_e$ is highly probable), appears to be much better than Eq. (11), and leads us to another method

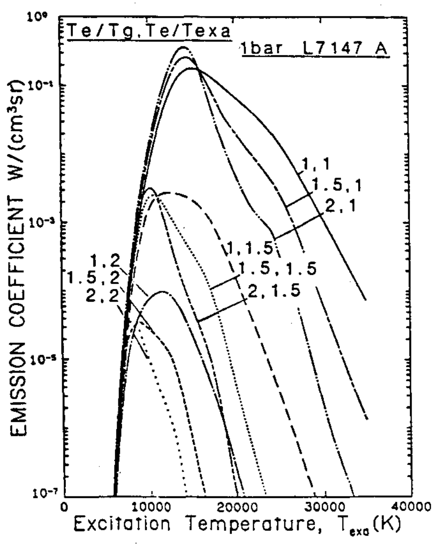

Fig. 2 Line emission coefficient for ArI 7147 at 1-bar for kinetic and excitation non-LTE.[7,9,12]

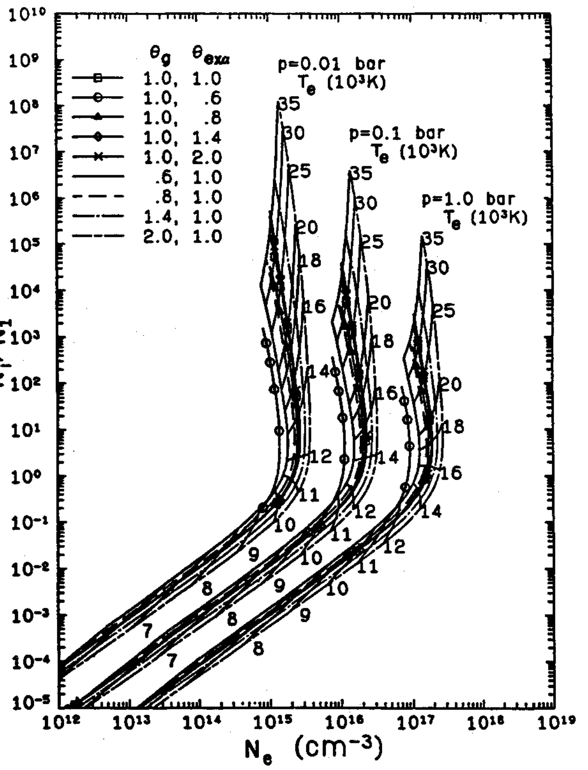

Fig. 3 GMTE state diagram for hydrogen plasmas at 0.01, 0.1, and 1.0 bar.[7,10]

(TETG) which is valid at higher temperatures as discussed later.

Diagnostic Methods

Diagnostic methods can be classified as low-, medium-, or high-temperature methods. The low-temperature methods use one or more of the low-temperature approximations discussed above. They are useful when T_{exa} is sufficiently below $T_{exa,\mathrm{norm}}$. $T_{exa,\mathrm{norm}}$ is usually below, but may be above, $T_{\mathrm{LTE,norm}}$ depending on T_e/T_g and T_e/T_{exa}. For plasma thrusters the low-temperature methods may not be useful because of the high temperatures expected and, therefore, they will not be discussed here. The medium-temperature methods use the constraint that $N_e = N_i$ or $N_e = \Sigma_j N_{i,j}$ over chemical species j; hence, they span the normal peak to temperatures about 1.5 times T_{norm}. These methods are the focus of this paper. High temperature methods extend to multiple ionization, $N_e = \Sigma i N_i$, etc. They are not discussed here, but procedures would be similar.

The medium-T methods used here get N_e from the continuum (for line broadening or other methods), but all march by increasing T_e. T_e calculated from the GMTE Saha equation is relatively stable, so that the increasing, iterative T_e converges nicely, as long as sufficient steps are provided to overcome the history effect in densities and in the transport properties when energy equations are used. The march can continue above the temperature at which intensities (and/or N_e) peak ($>T_{\mathrm{norm}}$) to determine solutions. Additional details of methods of solution should be sought in the references.

Four medium-T methods are considered here: ARCS, TETG, JET-G, and JET-H. ARCS is for electric arcs or when the electric field strength is known and dominates the electron energy equation. TETG may be used for arcs or jets when $T_e = T_g$. The general evaluation procedure is as follows:

a) explicitly determine p, $T_{ex\beta}$ and N_l/g_l via Eqs. (2), (4); b) initialize unknown values, using LTE calculations based on $T_{\mathrm{LTE}}(N_m)$ and p; c) calculate N_e from the continuum, Eq. (5); d) march $T_e = T_e + \Delta T_e$; e) calculate T_g (see each program below); f) calculate N_a from state, Eq. (7); g) calculate T_{exa} from Boltzmann, Eq. (6); h) calculate $T_{e,\mathrm{calc}}$ from Saha, Eq. (8); i) interpolate for T_e for solution; j) recalculate N_e from continuum with new properties; k) reiterate until T_e (or N_e) converges.

The methods of determining T_g (Step e) for the medium-T programs are now discussed in order of increasing complexity. All require non-LTE partition functions at the proper pressure or densities.

TETG Program

TETG[15] uses $T_g = T_e$ for jets/plumes as suggested by the results from more complex programs applied near the torch exit in various experiments. The program runs rapidly because it is simple and does not use transport relations nor take temperature derivatives. It operates on data from one position or cross section. Its major limitation is the assumption that $T_g = T_e$. It is also used to get rapid first estimates of T_e and T_{exa} in the JET-H program.

JET-G Program

JET-G[15] uses the difference between the electron and gas energy equations, assuming negligible enthalpy change (fully developed enthalpy profile) to estimate the maximum $T_e - T_g$ difference. For a fully developed flow/energy condition $\Delta H = 0$; hence, Eq. (9) can be written as

$$-Q_{eg} = C_{eg}(T_g - T_e) = Q_{e-\mathrm{cond}} + Q_{e-\mathrm{amb}} + Q_{e-\mathrm{rad}} + W_e \tag{14}$$

or

$$T_g - T_e = -(Q_{e-\mathrm{cond}} + Q_{e-\mathrm{amb}} + Q_{e-\mathrm{rad}} + W_e)/C_{eg} \tag{15}$$

The equation is in the form of heat generation per unit volume; therefore, C_{eg} is a specific heat generation coefficient (per unit volume). Since this is the electron energy equation, if the Q terms are negative (energy flow out), then $T_g - T_e > 0$ because the only "external" source of energy is the gas via $C_{eg}T_g$ and/or the "internal" energy $C_{eg}T_e$. We can consider the gas as a thermal reservoir at T_g. The depression of T_e from this reservoir temperature is then

$$T_e - T_{g,\mathrm{res}} = +(Q_{e-\mathrm{cond}} + Q_{e-\mathrm{amb}} + Q_{e-\mathrm{rad}} + W_e)/C_{eg} \tag{16}$$

Similar arguments can be made using the gas energy equation such that the depression of the gas temperature from the electron thermal reservoir is

$$T_g - T_{e,\mathrm{res}} = +Q_{g-\mathrm{cond}}/C_{eg} \tag{17}$$

If the loss of energy from the unit volume is the same for both electrons and gas, then the temperature depressions will be the same. If the effective reservoir temperatures (initial $T_e - T_g$) were the same, then $T_e = T_g$ results. By taking the difference in the energy transfer, we get an estimate of the maximum difference in $T_e - T_g$

$$(T_e - T_g)_{\max} = (T_e - T_{g,\mathrm{res}}) - (T_g - T_{e,\mathrm{res}}) \tag{18}$$

This is a maximum because the ΔH terms in Eqs. (9) and (10) decrease the magnitude of the terms in Eqs. (16) and (17).

The JET-G program takes much longer to run than TETG and has more problems converging at large radii with steep gradients. It has the advantage of being a one-position program and gives a good indication whether or not $T_g = T_e$, but overestimates the difference.

JET-H Program

JET-H[15] uses the electron energy equation, including ΔH_e from two different cross sections, to determine $T_e - T_g$. Rearranging Eq. (9) to get $T_e - T_g$ gives

$$T_e - T_g = (Q_{e-\mathrm{cond}} + Q_{e-\mathrm{amb}} + Q_{e-\mathrm{rad}} + W_e - \Delta H_e)/C_{eg} \tag{19}$$

from which T_g can be found for each T_e while marching. In this program, TETG is used to estimate N_e, T_e, T_{exa}, etc. at Axial Position 1 and then at Axial Position 2; then, subroutine JET-H averages this information and calculates $T_e - T_g$ via Eq. (19). After convergence, $T_e - T_g$ is input to the TETG program again at Positions 1 and 2 to reevaluate N_e from the continuum, T_e, etc., then back to JET-H to recalculate $T_e - T_g$. All iterations are stopped when T_e converges between programs.

One of the major problems is to get good velocity values, $u(r)$, in order to calculate the enthalpy rates in Eqs. (9) and (10). In the JET-H results presented below, the velocity profile was assumed similar to the temperature profile. The maximum velocity was obtained from a calculation by Vardelle[21] which uses the nozzle diameter, flow rate, power into the gas, and the temperature profile. In plasma jets near 1-atm, ΔH_e has effectively cancelled any $T_e - T_g$ effect predicted by JET-G.

This program takes a long time to run, about 2 h on an HP 216. Both the JET-G and JET-H programs require electron and gas transport properties and electron total radiation.

ARCS Program

ARCS[7,9,12,15] uses the electron energy equation at one position (without ΔH_e) to determine $T_e - T_g$. This method is valid for fully developed flow and energy profiles, since $\Delta H = 0$. It, therefore, requires a significant energy source such as the electric field to make up the energy losses. The equation for $T_e - T_g$ is identical to Eq. (19) with $\Delta H_e = 0$. The program takes about 1 h to run on an HP 216 with about six iterations over N_e, of which the last three are almost identical. The ARCS program requires electron (not gas) transport properties.

Experimental Results

Constricted Arcs

The ARCS program was applied to a 30 A, 3 mm diameter, wall-stabilized argon arc at various pressures from 0.1 to 10 bar.[7,9,12] Intensities of up to nine ArI lines were used to determine $T_{ex\beta}$ and N_l/g_l. Absorption was corrected for and both strong and weak lines were used to check the absorption correction. Stark broadening of $H\beta$ (<1% H concentration) was corrected to the 2-λ scale[22] to get accurate N_e. Using A_{mn} from NSRDS-NBS-22,[23] the various temperatures were obtained[12] as shown in Fig. 4. With corrected A_{mn},[7] the error bars decreased by more than a factor of two and $T_{ex\beta}$ comes into equilibrium with the other temperatures at high pressures.

It is surprising that $T_e < T_{exa}$ until one realizes that in this particular regime resonance radiation is still trapped, providing most of the excitation is to the first level, but heat conduction and radiation losses are reduced at the low pressures; hence, less energy is required from the electric field and T_e may drop below the resonance radiation temperature (which is approximately T_{exa}). An opposite effect is shown in high-power jets, below, in which the same ARCS program has been used for comparison. Details of this experiment are published elsewhere.[9]

Arc in a Rotating Magnetic Field

Another experiment applied the ARCS diagnostics program to a 1-atm, 350 A, argon arc which rotated in concert

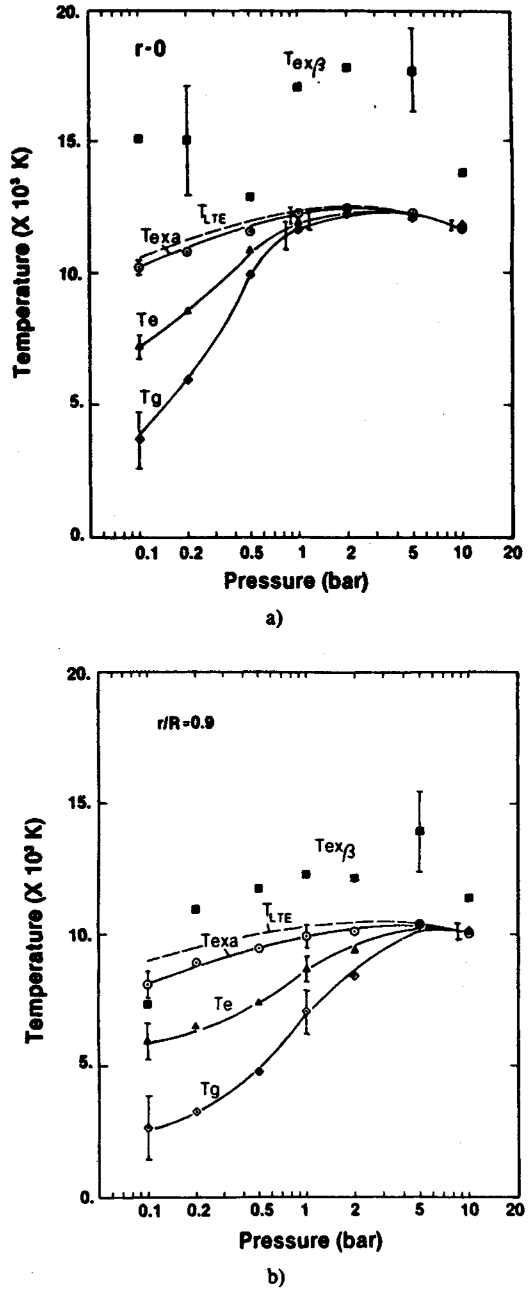

Fig. 4 $T(p)$ plot from a 30 A, 3-mm-diameter, low-flow, argon, wall-stabilized arc.[7,9,12]

at 1000 Hz with a rotating magnetic field (RMF)[13,14,24] with 100 and 200 G field strengths. The arc rotates in a 50-mm diameter channel. Five ArI lines plus $H\beta$ (<1% H concentration) intensities were measured to get $T_{ex\beta}$, N_l/g_l, and N_e, as above. Results for the 200 G condition are shown in Fig. 5. The relationship of the temperatures is identical to those in Fig. 4 at 1-atm, but with lower values. The 100 G case gives identical values to Fig. 5, except $T_{ex\beta}$ is 25,000 to 40,000 K. The zero magnetic field case is the same as the 200 G case. The 100 G case represents the maximum of the phenomenon called spectral line amplification. The study[14] found that N_e and the temperatures other than $T_{ex\beta}$ were identical in both cases; hence, many of the proposed reasons for spectral line amplification were found to be false. Fig. 5 shows another reason why $T_{ex\beta}$ should not be equated to T_e.

Plasma Jets

In France, argon plasma torches were operated in a chamber filled with argon at 1-atm and currents of 285 and 527 A.[15] The ARCS program was rewritten for an HP 216 and

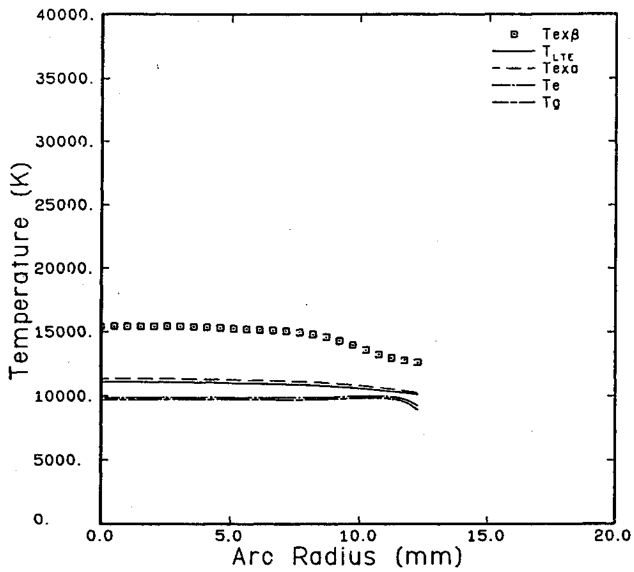

Fig. 5 ***T(r)* plot of a 350 A, argon arc in a 200 G magnetic field rotating at 1000 Hz.[13,14]**

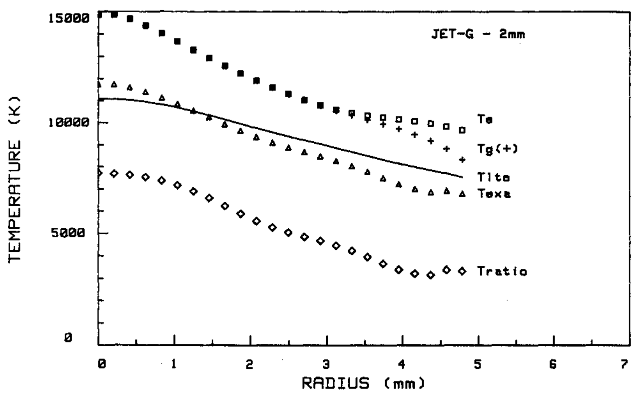

Fig. 6 ***T(r)* plot for an argon plasma torch jet, 285 A at z = 2 mm from the exit, obtained using the JET-G analysis.[15]**

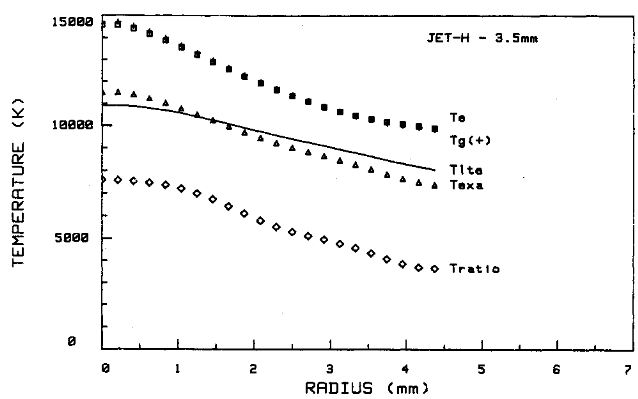

Fig. 7 ***T(r)* plot for the 285 A, plasma jet, z = 3.5 mm, from the JET-H analysis.[15]**

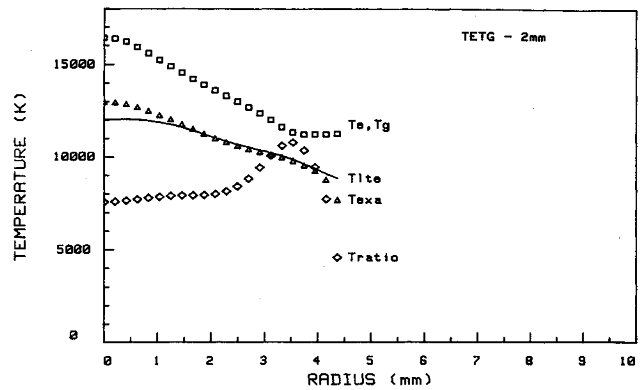

a) z = 2 mm

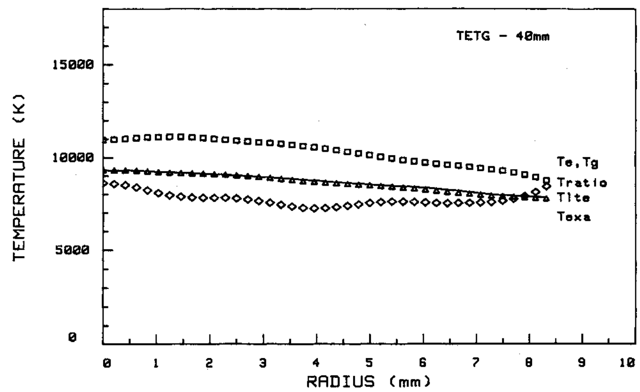

b) z = 40 mm

Fig. 8 ***T(r)* plot of a 527 A, argon plasma torch jet, from the TETG analysis.[15]**

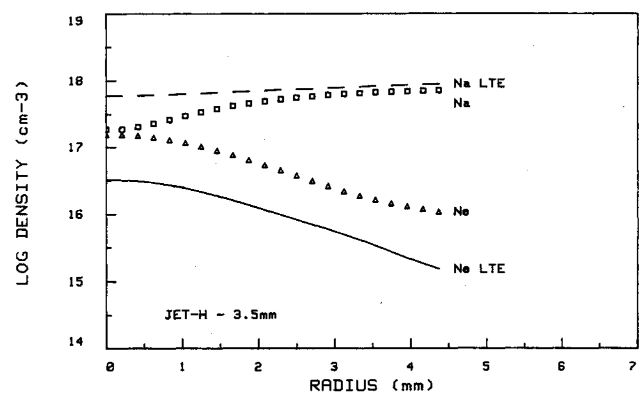

Fig. 9 ***N(r)* plot for the 285 A, argon jet, z = 3.5 mm, from the JET-H analysis.[15]**

applied to plasma jet measurements assuming electric field strengths of 0, 0.5, and 5 V/cm. In this case, a GMTE, non-LTE continuum relation was used to determine N_e and 4 to 6 lines were used. Only the 5 V/cm assumption produced $T_e > T_g$ at large radii, with equality over most of the jet. The results of the JET-G program shown in Fig. 6 were similar to the results of the ARCS program which used 5 V/cm. The more accurate JET-H program removed this inequity, obtaining $T_e = T_g$, as shown in Fig. 7. The JET-H results at 285 A are identical to the TETG program results; TETG results for 527 A and Position 2 and 40 mm downstream are shown in Fig. 8. Downstream temperatures approach LTE but not as rapidly as expected.

Note that $T_e/T_g = 1$, but $T_e/T_{exa} \simeq 1.25$ near the nozzle exit. Note in Fig. 2 that the peak or normal point emission coefficient decreases almost a factor of 10 for this condition. Calculations assuming the LTE (1,1) curve in Fig. 2 will give a maximum $T_{\rm LTE}$ of about 11,000 K for emission coefficients that are actually peaking in this non-LTE condition.

The evidence of peaking is shown in the density plots in Figs. 9 and 10a for 285 and 527 A, respectively. In the first, peaking is just being approached because N_e just equals N_a on the axis. In the second, at double the current, N_e exceeds N_a by a factor of four. Note that the non-LTE and LTE densities are significantly different near the plasma center.

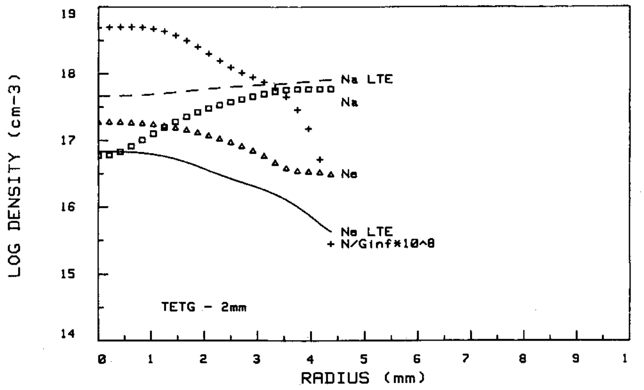

a) z = 2 mm

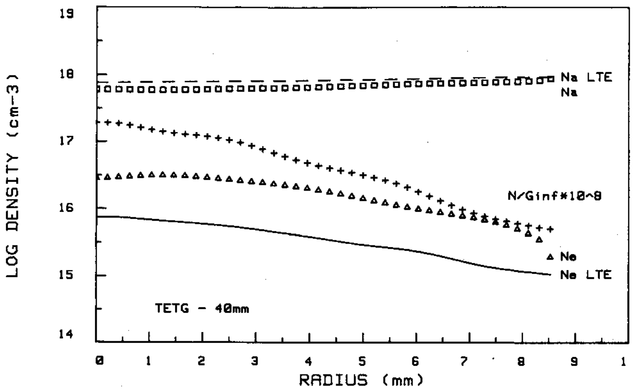

b) z = 40 mm

Fig. 10 $N(r)$ plot of the 527 A, argon jet, from the TETG analysis.[15]

LTE values are based on the highest level line absolute emission coefficient and the known pressure. Downstream at 40 mm, N_e remains large compared to LTE, as shown in Fig. 10b.

Conclusions

From the results, it appears that in low-pressure, low-flow arcs, T_e may be less than $T_{exa} \simeq T_{\mathrm{LTE}}$ because the trapped radiation does not need much help to maintain ionization. In high-power, high-flow, plasma jets, T_e equals T_g but is larger than T_{exa}, apparently to make up for the concentrated and increased energy loss rates. These results were obtained with the identical ARCS program and, for the jet analysis, were confirmed using various field-free programs. For the jets, the only difference was the use of the continuum for N_e, which may overestimate the N_e value. Nevertheless, even LTE analyses of the continuum indicate significantly larger values than N_e based on T_{LTE} from absolute line intensities.

Of generic diagnostic significance here is that the non-LTE diagnostic methods on jets using different principles (JET-G, JET-H, and TETG) gave almost identical N_e and T_e values and, over most of the radius, gave almost identical T_g values.

The major questions remaining in application to space propulsion plasmas are the following: Is the ion excitation temperature, T_{exi}, really equal to T_{exa} as assumed in Eq. (8)? Are the A_{mn} for (argon) ions sufficiently well known to judge the true effect? Why is there such a large discrepancy between theoretical and high-pressure experimental ξ_{fb} in argon at $\lambda > 450$ nm and how does that influence the use of continuum diagnostics in general? How do T_g measurements from Rayleigh scattering and Doppler broadening compare with values calculated from methods presented here? In low-pressure plumes are other temperatures necessary, e.g., $T_i \neq T_a \neq T_g$?

Acknowledgments

Without the excellent experimental work by A. Sedghinasab, R. V. Frierson, Ph. Roumilhac, and J. M. Leger, and the vision and support of P. Fauchais, this summary would not have been possible. The preparation of this paper was supported by the U.S. Department of Energy under DOE Contract DE-AC07-76ID01570.

References

[1] Eddy, T. L., "Electron Temperature Determination in LTE and Non-LTE Plasmas," *Journal Quantitative Spectroscopy Radiative Transfer*, Vol. 33, 1985, pp. 197–211.

[2] Bates, D. R., Kingston, A. E., and McWhirter, R. W. P., "Recombination between Electrons and Atomic Ions, I: Optically Thin Plasmas," *Proceedings of the Royal Society*, Ser. A, Vol. 267, May 1962, pp. 297–312, and "Recombination between Electrons and Atomic Ions, II: Optically Thick Plasmas," *Proceedings of the Royal Society*, Ser. A, Vol. A270, Nov. 1962, pp. 155–167.

[3] Braun, C. G., and Kunc, J., "Collisional-Radiative Coefficients from a Three-Level Atomic Model in Nonequilibrium Argon Plasmas," *Physics of Fluids*, Vol. 30, 1986, pp. 499–509.

[4] Cho, K. Y., and Eddy, T. L., "Collisional-Radiative Modeling with Multitemperature Thermodynamic Models," *Journal Quantitative Spectroscopy Radiative Transfer*, Vol. 41, 1988, pp. 287–301.

[5] Griem, H. R., *Plasma Spectroscopy*, McGraw-Hill, New York, 1964.

[6] Eddy, T. L., and Heberlein, J. V. R., *NSF Workshop on Thermal Plasma Systems*, Georgia Institute of Technology, Atlanta, GA, 1987, p. 105.

[7] Eddy, T. L., Sedghinasab, A., Cho, K. Y., Frierson, R. V., and Murray, R. T., "Radiative Properties of Non-Local Thermal Equilibrium Plasmas," NSF Grant CPE-8311325 (1987).

[8] Gleizes, A., Kafaroni, H., Dang Duc, H., and Maury, C., "The Difference between the Electron and the Gas Temperature in a Stationary Arc Plasma at Atmospheric Pressure," *Journal Physics D*, Vol. 15, 1982, pp. 1031–1054.

[9] Eddy, T. L., and Sedghinasab, A., "The Type and Extent of Non-LTE in Argon Arcs at 0.1–10 Bar," *IEEE Transaction Plantary Science*, Vol. 16, 1988, pp. 444–452.

[10] Cho, K. Y., "Nonequilibrium Thermodynamic Models and Applications to Hydrogen Plasma," Ph.D. Dissertation, Georgia Institute of Technology, Atlanta (1988).

[11] Cho, K. Y., and Eddy, T. L., "Radiative and Diffusional Effects to the Population Densities of the Excited-State Atoms in Hydrogen Plasma," *Review of Scientific Instruments*, Vol. 59, 1988, pp. 1524–1526.

[12] Sedghinasab, A., "Experimental Determination of Argon Atomic Transition Probabilities using Non-LTE Diagnostics," Ph.D. Dissertation, Georgia Institute of Technology, Atlanta, 1987.

[13] Frierson, R. V., and Eddy, T. L., "Temperatures in an Arc Nozzle Produced by a Rotating Magnetic Field," *Proceedings International Symposium of Plasma Chemistry*, Vol. 1, 1987, pp. 334–339.

[14] Frierson, R. V., "Spectroscopic Diagnostics of a Plasma in a Rotating Magnetic Field," M.S. Thesis, Georgia Institute of Technology, Atlanta, 1988.

[15] Eddy, T. L., Condert, J. F., Roumilhac, Ph., Leger, J. M., and Fauchais, P., "Non-LTE Temperature Determination in Atmospheric and Sub-Atmospheric Plasma Jets for Spraying." Final report, Laboratoire Ceramiques Nouvelles, Univ. Limoges, France, 1988.

[16] Eddy, T. L., Cremers, L. J., and Hsia, H. S., "The MTE Continuum Relation with Application to an Argon Arc at Atmospheric Pressure," *Journal Quantitative Spectroscopy Radiative Transfer*, Vol. 17, 1977, pp. 287–296.

[17] Biberman, L. M., and Norman, G. E., "On the Calculation of Photoionization Absorption," *Optics and Spectroscopy*, Vol. 8, 1960, pp. 230–232.

[18] Schluter, D., "Die Emissionskontinua Thermischer Edelgasplasmen," *Zeitscrift für Physik*, Vol. 210, 1968, pp. 80–91.

[19] Bauder, U., "Radiation from High-Pressure Plasmas," *Journal of Applied Physics*, Vol. 39, 1968, pp. 148–152.

[20]Eddy, T. L., "Critical Review of Plasma Spectroscopic Diagnostics Via MTE," *IEEE Transactions Plantary Science*, Vol. 4, 1976, pp. 103–111.

[21]Vardelle, A., University of Limoges, personal communication, 1988.

[22]Baessler, P., and Kock, M., "An Interferometric and Spectroscopic Study on a High-Current Argon Arc," *Journal of Physics B*, Vol. 13, 1980, pp. 1351–61.

[23]Wiese, A. L., Smith, W. M., and Miles, B. M., "Atomic Transition Probabilities," Vol. II, NSRDS-NBS-22, U.S. Government Printing Office, Washington, DC, 1969.

[24]Frierson, R. V., Eddy, T. L., and Put'ko, V. F., "Facility for Non-LTE Studies of a Magnetically Rotated Arc," *Review of Scientific Instruments*, Vol. 57, 1986, pp. 2096–2098.